Assembly of planar array components using anisotropic conducting adhesives: a benchmark study. Part II - theory

Assembly of Planar Array Components Using Anisotropic Conducting Adhesives—A Benchmark Study: Part II—Theory

Samjid H. Mannan, David C. Whalley, Adebayo Oluyinka Ogunjimi, and David J. Williams

***Abstract*— This paper presents new results from an experimental and theoretical program to evaluate relevant process parameters in the assembly of a 500 μm pitch area array component using anisotropic conductive adhesive (ACA) materials. This experimental configuration has features of micro ball grid array (μBGA) chip scale packaging (CSP) and also flip-chip and conventional ball grid array (BGA) package structures. The paper presents the results of computational fluid dynamics (CFD) models of the early stages of the assembly process when the adhesive is squeezed out between the device and the substrate. Experimental results on the assembly trials are presented in an accompanying paper [1] and have been previously reported at the Adhesives in Electronics Conference, Gothenburg, 1996 [2]. The CFD models outlined here show how those results might be expected to change for smaller pitches.**

***Index Terms*—Anisotropic conductive adhesive, computational fluid dynamics, flip-chip assembly.**

I. Introduction

ANISOTROPIC conducting adhesives [3], [4] typically consist of a dilute suspension of conducting particles in an adhesive resin. During assembly the resin is squeezed out of the gap between device and substrate by the application of heat and force. computational fluid dynamics (CFD) is being used in order to more fully understand this squeezing process, and how to optimize the bump device on the component to maximize the numbers of particles contributing to conduction across the gap. In this paper we use a commercially available CFD software package; Fidap 7.52. The main aim of the CFD studies undertaken so far have been to predict which pad shapes and surfaces will trap the maximum number of conducting particles, and how the pad layout affects the time taken to squeeze out the adhesive.

The CFD modeling has also been successful in refining previous analytical models [5] by taking into account the detailed geometry of the assembly (square versus circular chips, staggered pads, array pads etc.). The basic equation that has been used to model the flow analytically is termed the Scott equation [6]

$$\frac{dh}{dt} = -\frac{n}{2n+1}\left(\frac{F(n+3)h^{2n+1}}{2\pi\eta_0 R^{n+3}}\right)^{1/n} \tag{1}$$

and this relates the velocity that the adhesive is squeezed out at to the applied force, F, the radius of the chip, R, the gap between chip and substrate, h, and the viscosity of the adhesive where a non-Newtonian [6] power law model is assumed for the adhesive viscosity, η

$$\eta = \eta_0(\dot{\gamma})^{n-1} \tag{2}$$

$\dot{\gamma}$ is the shear rate in the fluid and n and η_0 are constants unique to each adhesive. This equation applies only to circular chips,

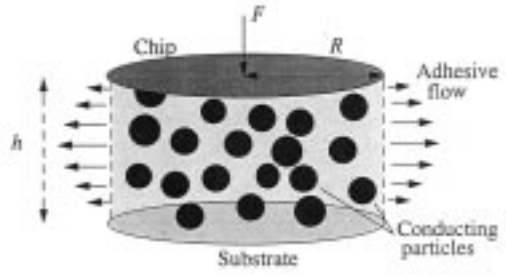

Fig. 1. Sketch of the anisotropic conductive adhesive (ACA) assembly process with flat circular chip and substrate.

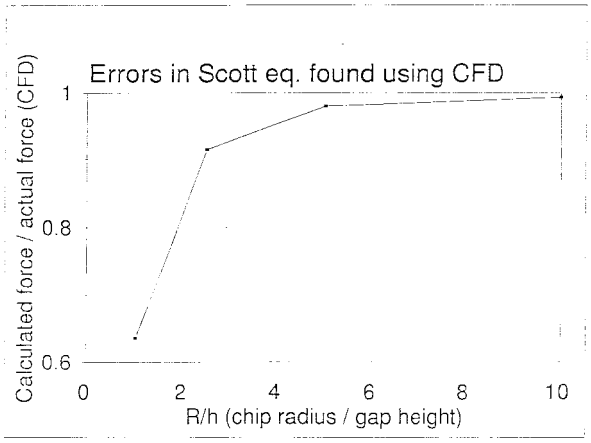

Fig. 2. Error in the force predicted by the Scott equation compared to the force predicted by CFD as the ratio R/h is decreased.

Manuscript revised November 1996. This paper was supported by Engineering and Physical Sciences Research Council (EPSRC) Contract GR/J68410 and a consortium of industrial partners which include, Cooksons Technology Centre and their associated company Alpha Metals Advanced Products, Eltek Semiconductors Ltd., Lucas Electronics, Rolls-Royce Plc, Design 2 Distribution Ltd., IBM (UK) Ltd., and Mitel Telecom. This paper was presented at the 2nd International Conference "Adhesives in Electronics," Stockholm, Sweden, June 3–5, 1996.

The authors are with the Department of Manufacturing Engineering, Loughborough University, Leics, LE11-3TU UK.

Publisher Item Identifier S 1083-4400(96)01528-8.

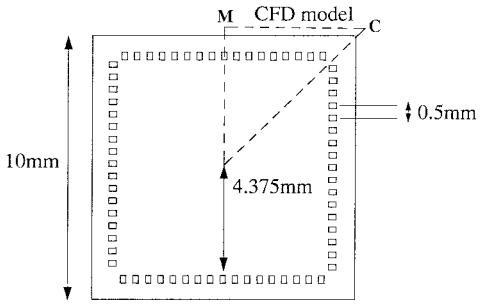

Fig. 3. Sketch of pads at the periphery of the chip and the segment of the chip required for CFD modeling.

and flat (i.e. unbumped) substrates and lands, as depicted in Fig. 1.

The other major assumption required for this equation to be valid is that the size of the chip be much larger than the gap between chip and substrate: $R \gg h$. Using CFD however it is possible to see exactly when this approximation breaks down. Fig. 2 shows the discrepancy between the Scott equation (with n set equal to 1) and the CFD prediction as the ratio R/H is reduced. It is seen that when R/h is larger than 10, the equation can still be used, while it cannot be used if the ratio is smaller than 2 with any degree of confidence.

In this simple application of CFD we have still retained flat surfaces for the chip and substrate. The real advantage of CFD however is that it can deal with bumped geometries. We are particularly interested in the case that the chip is bumped and that the substrate is relatively flat since this allows us to predict the effects of the bumps on fluid flow, and hence the CFD models will retain flat substrates. This limitation can be removed if required. Also to simplify the models we will retain the simplest fluid model, a Newtonian fluid, with n set equal to 1 in (2), but non-Newtonian fluids can be easily modeled if desired. One advantage of using a Newtonian fluid model is that the flow patterns remain unchanged whatever the force applied to the chip (assuming laminar flow); if the force is increased by a factor of 2, then all the velocities are also doubled.

The models will show the paths taken by infinitesimally small conducting particles. Real conducting particles of finite size will effect the flow of fluid around them, and hence the CFD models will not be able to track the movement of particles exactly—account must be taken of mechanical and frictional forces between particles and surfaces for completely accurate predictions of particle motion and this is beyond the scope of any commercial CFD package. Nevertheless, the analysis of fluid flow without finite size conducting particles present leads to insight as regards the case when the particles are present.

II. Effect of Pad Pitch and Layout on the Chip

CFD has been used to explore the effects of reducing pad pitch and pad layout on the chip from the 500 μm pitch used in the benchmark experiments [1], [2] to 200 μmand 100 μm pitches relevant to current and future generation flip chip devices. A number of variations on the benchmark geometry are now examined.

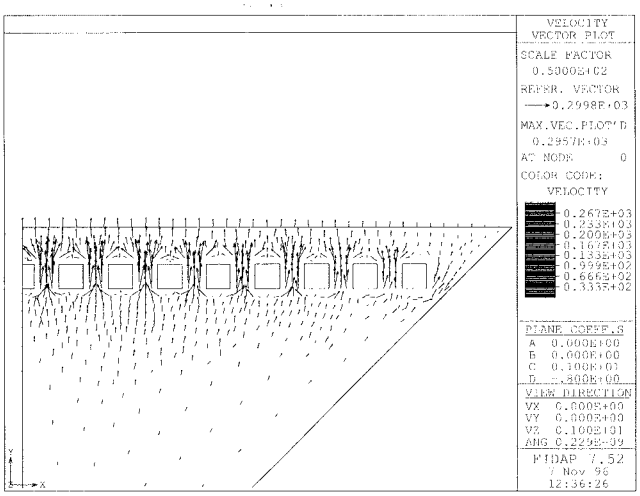

Fig. 4. Flow pattern predicted by CFD around the bumps sketched in Fig. 3.

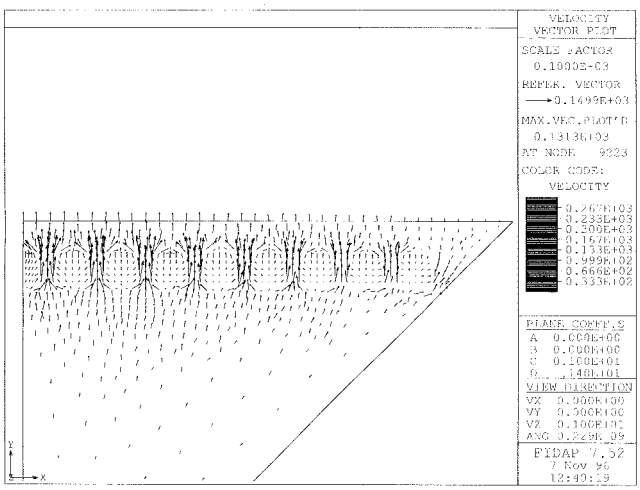

Fig. 5. Flow pattern predicted by CFD over the bumps sketched in Fig. 3.

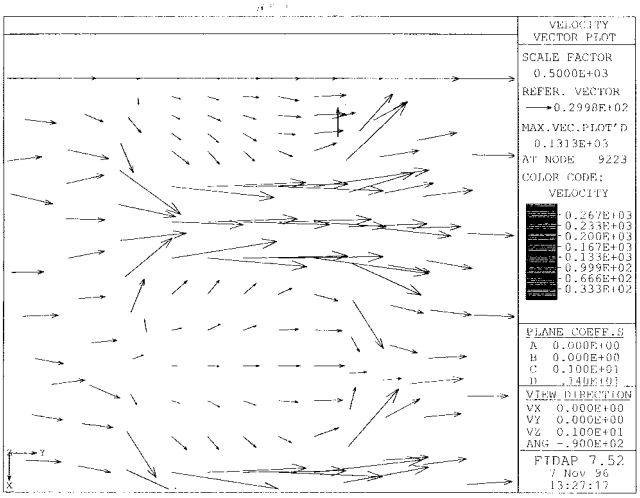

Fig. 6. Expansion of Fig. 5 for the pads furthest from the corner.

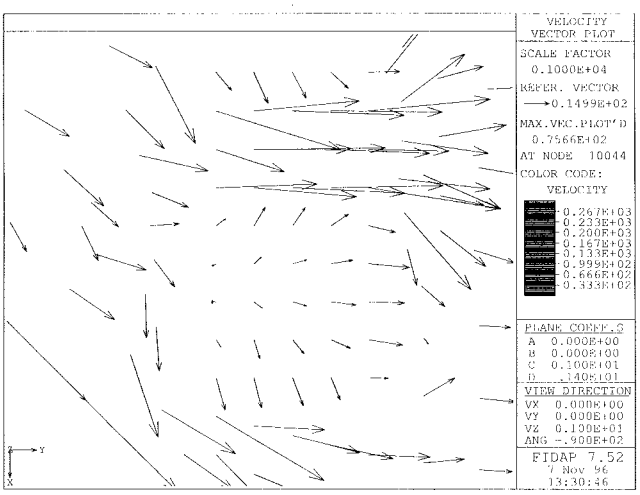

Fig. 7. Expansion of Fig. 5 for the corner pad.

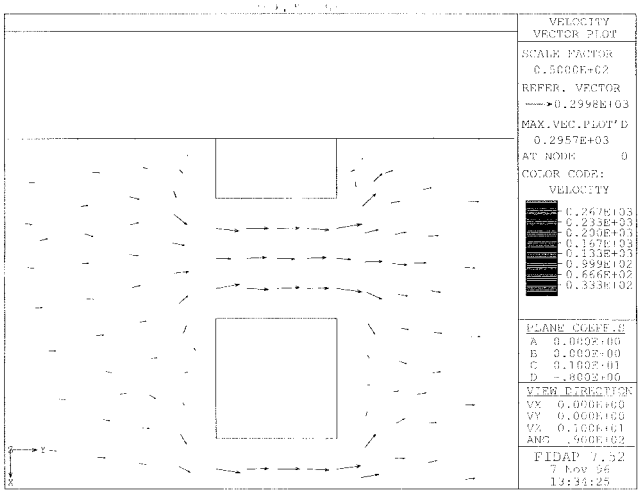

Fig. 8. Expansion of Fig. 4 for the pads furthest from the corner.

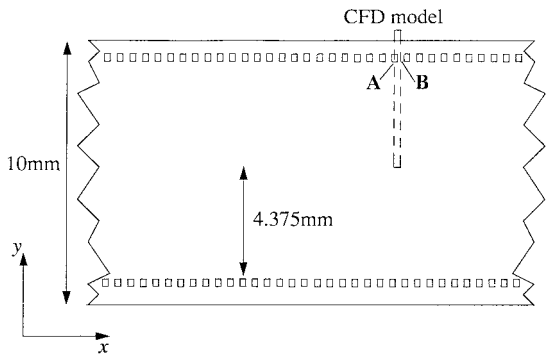

Fig. 9. Sketch of a section of an infinitely long chip with the pads at the periphery, and the CFD segment required for CFD modeling.

A. Square Pads at the Periphery of the Chip at 500 μm Pitch

CFD models have been constructed for flow around pads at 250 μm, 100 μm, and 50 μm square land sizes and 500 μm, 200 μm and 100 μm pitches, respectively. The pad heights have been kept at 30 μm in all cases, and it is assumed that the original thickness of the adhesive layer was such that all entrapped air has been expelled. This has previously been termed type II flow [5].

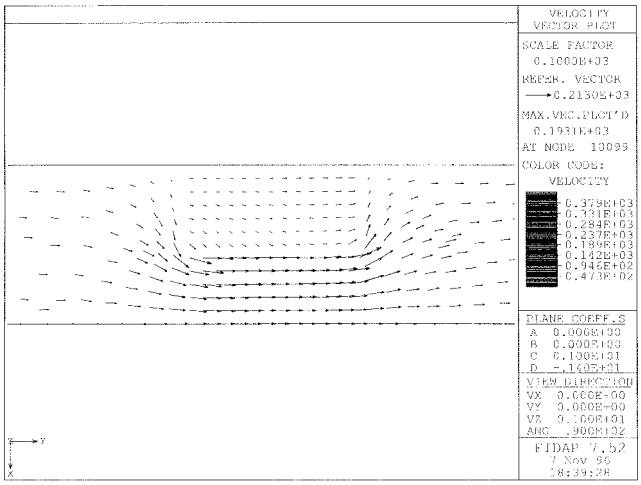

Fig. 10. Flow of fluid over the bumps sketched in Fig. 9 at 500 μm pitch.

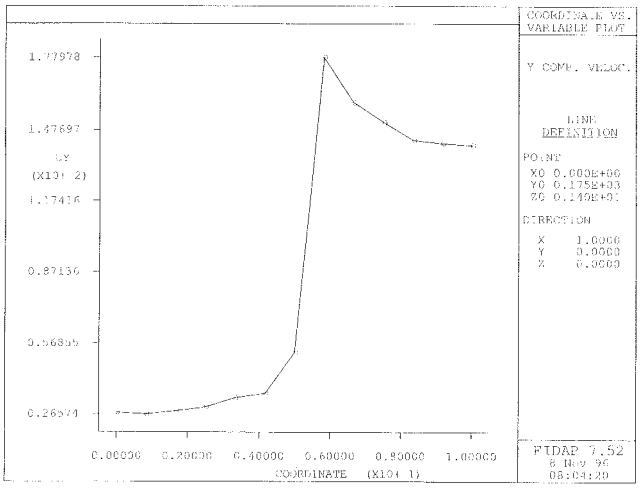

Fig. 11. Graph of the y component of fluid velocity across the line ***AB*** indicated in Fig. 9 for 500 μm pitch pads. The units on the x axis are such that 1 unit = 25 μm. The units on the y axis are arbitrary. The pad occupies the first 5 units (125 μm) and the channel between pads the last 5 units.

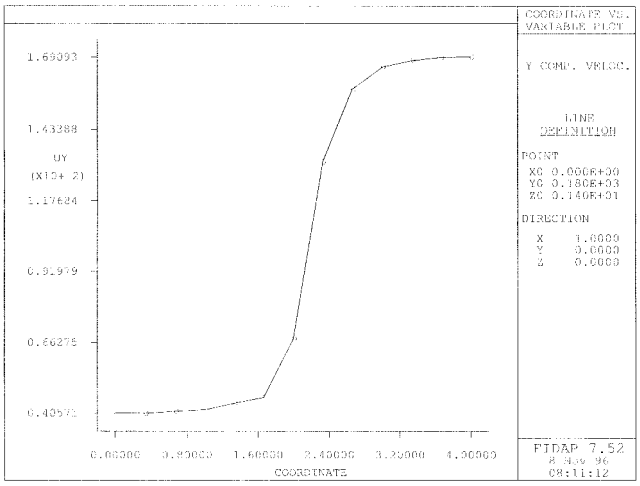

Fig. 12. As Fig. 11 but for 200 μm pitch pads.

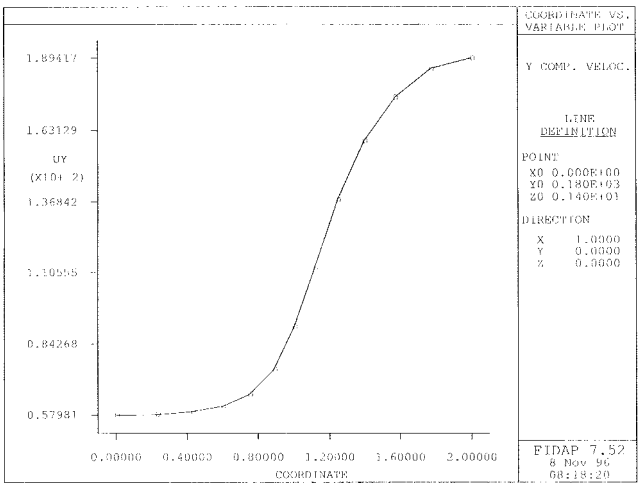

Fig. 13. As Fig. 11 but for 100 μm pitch pads.

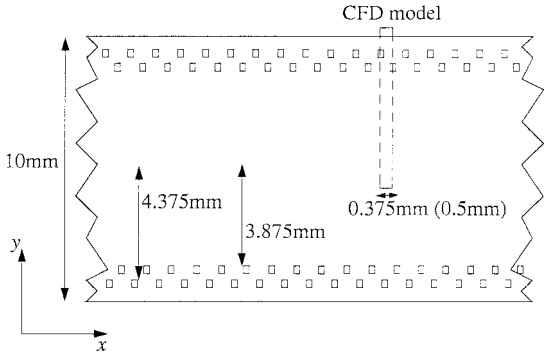

Fig. 14. Sketch of staggered 500 μm square pads at 375 μm (or 500 μm) pitch.

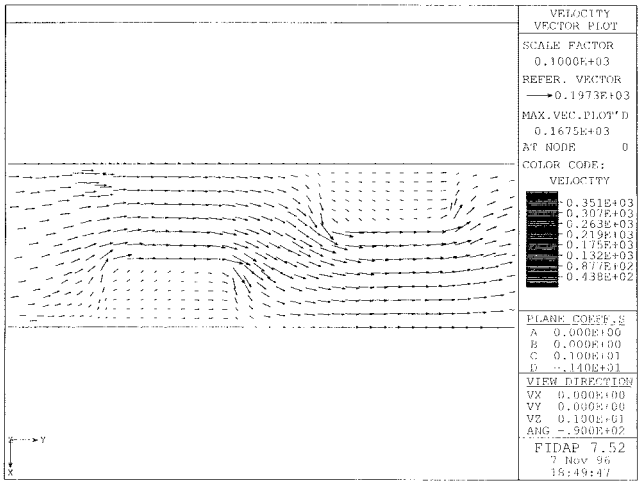

Fig. 15. Flow of fluid over the bumps sketched in Fig. 14 at 375 μm pitch.

We examine first the 500 μm pitch model as this approximates the benchmark experiment [1], [2] geometry most closely. Fig. 3 shows the geometry assumed for the model.

Due to the symmetries of the square we need model only the triangle indicated by Fig. 3 in order to get the full flow pattern. The results of the CFD model for the velocity flow

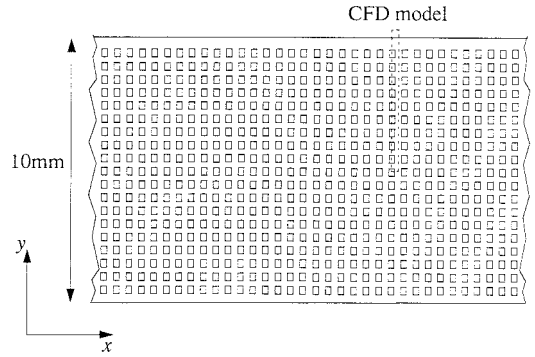

Fig. 16. Sketch of area array device at a pitch of 500 μm and the segment required for CFD modeling.

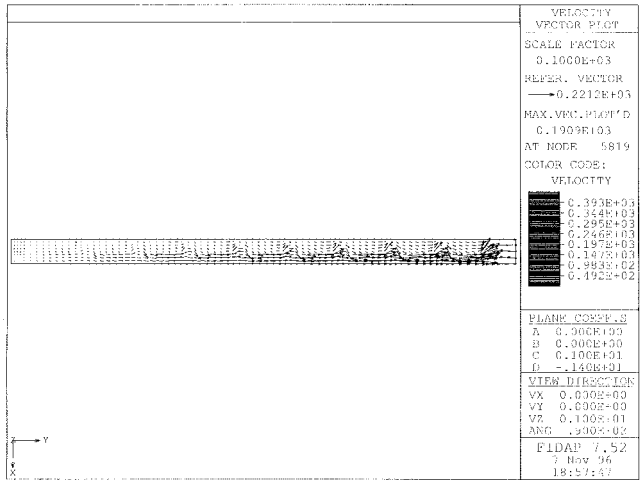

Fig. 17. Flow of fluid over the bumps sketched in Fig. 16.

field in the case when the substrate is 10 μm from the bumps (40 μm from the chip surface) is shown in Fig. 4 in a plane parallel to the substrate and 20 μm from it. In Fig. 5 we see the flow field in a plane 5 μm from the substrate—the positions of the pads are clearly marked by regular arrays of velocity vectors over the pad positions.

These figures show that there is insignificant flow out of the corners of the chip—the bulk of the adhesive will flow out near the midpoint of the edges (marked $\boldsymbol{M}$ in Fig. 3) rather than the corners (marked $\boldsymbol{C}$ in Fig. 3). Experimentally this is the pattern that is observed, with the volume of displaced adhesive at a maximum at $\boldsymbol{M}$, and a minimum at $\boldsymbol{C}$.

The most important aspect of the predicted flow patterns is whether there is flow over the bump or around it. Flow over the bumps is considered undesireable compared to flow around the bumps because flow off the pad is thought more likely to remove particles from the pad than for the flow onto the pads to replenish them. This is because the edges of the bumps will obstruct a large proportion of the incoming particles. Furthest from the corner it is seen that the flow is over the pad (Fig. 6), while at the corner, the flow is around the pads to a much greater extent (Fig. 7). This may result in a higher density of particles on the pads nearest the corners. During the benchmark trials [1], [2] there were in fact a greater number of opens at

the corners, suggesting that the effects of angular misalignment of chip and substrate dominated in that experiment.

One unexpected result is that the flow in the channel between pads is weaker in the middle of the channel between neighboring pads and stronger closer to the pad edges as is indicated by Fig. 8, which is an expanded view of a portion of Fig. 4. This is a consequence of the spacing between pads being much larger than the height of the channel, and not an artifact of the CFD mesh as has been verified by using a finer mesh. The effect is not reproduced for the smaller pads and spacings which we shall examine next.

B. Square Pads at the Periphery of the Chip at 200 μm and 100 μm Pitch

We are interested in how the flow patterns will change as we move toward finer pitches. As the pads become smaller, we would expect them to offer less resistance to the flow out from the centre of the chip and this is what is observed. We have already examined the effect of a square chip geometry in Section II-A, and henceforth we shall simplify matters by concentrating on a single pad. Fig. 9 shows the new geometry employed, which shows that we are now modeling an infinitely long chip, 10 μm wide, so that the flow over all the bumps is identical. Fig. 10 shows the flow field for the 500 μm pitch geometry when the substrate is 10 μm from the substrate (40 μm from the chip surface). Fig. 11 shows the y component of velocity across the pad 5 μm from the substrate across the line AB shown in Fig. 9.

We can now compare Fig. 11 against the flux of fluid onto the chip for the 200 μm and 100 μm pitch cases (100 μm and 50 μm square pads) which are shown in Figs. 12 and 13, respectively. In both cases the flow is over the chip to a far greater extent than for the 500 μm pitch device, resulting in a stronger tendency for the particles to be swept off the pads.

As the bump height is reduced the bumps will offer even less resistance to the flow in the final stages of compression. To see this consider the case of infinitesimal bump heights where the bumps offer zero resistance. However this does not necessarily mean that the flow over the pads will be stronger because the overall flow velocity will be reduced as is shown by (1). As the pitches and pad sizes reduce, the slow down of the overall flow scale will be the dominant effect and then small pad heights will be preferred. By contrast for the larger pads (of the order of 250 μm square) larger bump heights will reduce the flow over the pads in the final stages of compression.

C. Staggered Pad and Array Pad Geometries (250 μm Square Pads)

If the time taken to squeeze out the adhesive needs to be reduced, then staggered pads are one option that might be considered. Fig. 14 describes one possible arrangement, and Fig. 15 shows the flow pattern in this case. The pads are 250 μm square and 30 μm high as before.

We are also increased in area array devices, and one possible geometry is sketched in Fig. 16, with the flow pattern given by Fig. 17. In this case the pitch in both the x and y directions is set at 500 μm.

To achieve a given flux of fluid out from under the chip, a specified force must be applied to the chip. We can see how this force varies with different pad layouts. Compared to the case when there are no pads at all, the geometry indicated in Fig. 9 increases the required force by approximately 18% in the final stages of compression. For the staggered pad geometry at 500 μm pitch the increase is 15%, while at 375 μm pitch the increase is 19%. The fact that there appears to be comparatively little difference between such drastically different geometries is attributable to the large gap between pads compared to the gap between substrate and chip surfaces, which is also the factor responsible for the increased flow rate near the edges of the pad as previously discussed.

For the smaller 100 μm square lands (at 200 μm pitch in the geometry indicated by Fig. 9) the increased force is only 10%; it seems that smaller pads cause less resistance to flow despite there being more pads in total. This result is significant because it indicates that decreasing pitch and pad sizes will not increase process times.

However, for the area array at 500 μm pitch, the force required is larger by 97% i.e. nearly a factor of two. This should be regarded as a lower limit, because as Fig. 17 shows, the flow out from the center of the chip in the y direction is channelled into an unobstructed path. For a finite sized chip however, the flow will have a significant x component of flow, and will be forced to collide with the pads to a much greater degree, increasing the resistance to flow still further. The flow is observed to become over the pads increasingly out from the center line of the chip.

III. Conclusion

The models show that the use of anisotropic conductive adhesive (ACA) materials at finer interconnection pitches will not significantly effect the overall processing time, but that conducting particle depletion on the connection pads will become more of an issue due to the increased amount of adhesive flow over the pads.

The effect of different pad layouts has been examined, as well as the effect of having noncircular chip geometries. In particular it was pointed out that the flow out from the center of the chip will be much weaker at the corners, and the central regions of the chip, resulting in enhanced particle numbers in these regions.

References

[1] S. H. Mannan, D. C. Whalley, A. O. Ogunjimi, and D. J. Williams, "Assembly of planar array components using anisotropic conducting adhesives—A benchmark study: Part I—Experiment," this issue, pp. 264–269.

[2] ——, "Assembly of planar array components using anisotropic conducting adhesives—A benchmark study," in *Proc. Adhesives Electron.'96*, Stockholm, 1996, pp. 270–284.

[3] A. O. Ogunjimi, O. A. Boyle, D. C. Whalley, and D. J. Williams "A review of the impact of conductive adhesive technology on interconnection," *J. Electron. Manufact.*, vol. 2, pp. 109–118, Sept. 1992.

[4] J. H. Lau, Ed., *Flip Chip Technologies.* New York: McGraw-Hill, 1996, chs. 6–10, pp. 223–340.

[5] S. H. Mannan, D. C. Whalley, A. O. Ogunjimi, and D. J. Williams "Modeling of the initial stages of the anisotropic adhesive joint assembly process," in *Proc. 1995 Japan IEEE IEMTS*, Omiya, Dec. 4–6, 1995, pp. 142–145.

[6] J. R. Scott, *Trans. Inst. Rubber Ind.*, vol. 7, p. 169, 1931.

Samjid H. Mannan, for photograph and biography, see this issue, p. 263.

Adebayo Oluyinka Ogunjimi, for photograph and biography, see this issue, p. 263.

David C. Whalley, for photograph and biography, see this issue, p. 263.

David J. Williams, for photograph and biography, see this issue, p. 263.